Journal of
Ceramic Science
and Technology

J. Ceram. Sci. Technol. 1-8 (2019)
DOI: 10.4416/JCST2018-00041
available online at: http://www.ceramic-science.com

Graphite carbon enclosed AlN nanoparticles with enhanced methanol-tolerant electrocatalytic properties for oxygen reduction

C. Liang[1], H. Wang[*2], K. Huang[3], W. Liu[1], K. Bi[1], M. Lei[*1]

[1]State Key Laboratory of Information Photonics and Optical Communications & School of Science, Beijing University of Posts and Telecommunications, Beijing 100876, China
[2]Materials Science and Engineering Program and Texas Materials Institute, The University of Texas at Austin, Texas, 78712, United States
[3]State Key Laboratory of New Ceramics and Fine Processing, School of Materials Science and Engineering, Tsinghua University, Beijing 100084, China
received June 2, 2018; received in revised form February 1, 2019; accepted February 18, 2019

Abstract

The methanol crossover effects and high-cost of Pt based catalysts severely restrict the practical applications of direct methanol fuel cells (DMFCs). In this work, a novel structure of ~25 nm AlN nanoparticles with graphite carbon outer coating (AlN@C) was synthesized via a one-step solid-state method with simultaneous nitridation processes and carbon graphitization. AlN@C nanocomposites were exploited as a catalyst of the oxygen reduction reaction (ORR). Benefited from the graphite carbon outer coating, AlN@C exhibits enhanced electrochemical properties (more positive onset potential and higher current density) than pure AlN. Notably, superior methanol-tolerance (a negligible current change after adding 3 M methanol) and excellent durability (91.4 % of the initial current density remained after 10000 s of chronoamperometry test) can be observed. This study provides a feasible approach for developing the applications of traditional ceramic materials towards the ORR catalyst in DMFCs.

Keywords: Aluminum nitride, composite materials, graphite carbon, fuel cells, oxygen reduction reaction.

I. Introduction

To meet the growing energy demand, exploitation of new energy conversion devices has attracted much attention, because the traditional fossil fuels are limited in resource reserve and can result in severe environmental disruption [1–5]. Fuel cells have been considered as one of the most promising power source due to their high efficiency and low emission levels [6–8]. In particular, direct methanol fuel cells (DMFCs), which produce electrical energy from the electrochemical reactions of methanol oxidation and oxygen reduction, are more attractive for the portable electrical applications [9–12]. However, the cathodic oxygen reduction reaction (ORR) is still a primary factor to determine the reaction kinetics of DMFCs for its sluggish kinetics. Although the Pt based materials have been employed as state-of-the-art electrocatalyst, the high cost restricts their commercialization. In addition, the poisoning of cathode caused by detrimental effect of methanol crossover is another critical issue [12–14].

In order to overcome these problems, great efforts have been made to develop novel methanol-tolerant electrocatalysts. Pt-based alloy with transition metals non-active toward methanol oxidation, such as Co, Ni, Fe and Cu, is employed to enhance the ORR and methanol-tolerant performances [15–19]. Nevertheless, the unmanageable process for preparation of these nanocrystalline alloys and their inherently tendency to favor the methanol oxidation over ORR cannot satisfy the huge demand for low-cost and efficient methanol-tolerant catalysts [20]. Recently, various nitrogen coordinated non-precious metals have been demonstrated to possess high activity and methanol-tolerance for ORR. Compared to particular metal crystal, the metal nitrides with metal-nitrogen bonding on the surface is expected to be favorable for ORR activity due to the disordered lattice that can promote the donation of electrons to oxygen molecules [21]. The catalysts of FeN, NbN and TiN have been reported to exhibit positive onset potentials for the ORR close to those of Pt based materials [22–25].

Considering the superior electronic conductivity and strong toughness of carbon materials include graphene, carbon nanotubes and mesoporous carbons, developing the composites with these carbon materials is one of the most common strategies to improve the electrocatalytic performance [26–28]. For instance, the VN/C nanocomposites exhibit a considerable ORR activity with an approximate onset potential at about 0.87 V vs. RHE and an obviously superior methanol-tolerant performance comparing to the Pt/C catalysts [29]. Recently, Fe-N-doped mesoporous carbon microspheres are synthesized using a facile in situ replication and polymerization strategy and exhibit high activity, superior durability, and good tolerance to methanol in comparison to commercial Pt/C catalysts [30].

* Corresponding author: wanghao900111@utexas.edu, mlei@bupt.edu.cn

In this work, the novel AlN@C nanocomposites of AlN nanoparticles enclosed by graphite carbon are successfully synthesized via a one-step solid-state method employing melamine and Al_2O_3 as raw materials under N_2 atmosphere. The unique structure with graphite carbon outer coating ensures the enhanced current density, onset and half-wave potentials, long-time durability and methanol-tolerance of the AlN@C nanocomposites toward ORR. The results indicate that AlN@C nanocomposites can be a promising methanol-tolerant catalyst for ORR in DMFCs.

II. Experimental

All the raw materials are of analytical pure grade and purchased from commercial source without further purification. In the typical synthesis of the AlN@C nanocomposites, 5 mmol Al_2O_3 powder and 40 mmol melamine ($C_3N_3(NH_2)_3$) were mixed together, followed by being milled to homogeneity in an agate mortar. Then, a certain amount of the obtained mixture should be transported to the steel mold and was pressed into tablets. These tablets were heated at 1500 °C for 12 h with a heating rate of 5 K/min in the high temperature tubular furnace (GXL-1700X). After cooling to room temperature, the black AlN@C powders were collected. To isolate the air, a steady flow of N_2 at 50 sccm was conducted in the whole heating and cooling processes.

The X-ray diffraction (XRD) pattern was collected on the Panalytical X'pert diffractometer from 10° to 90° with Cu Kα radiation. Micro morphology and structure were characterized by the field-emission scanning (FESEM, Hitachi, S-4800) and transmission electron microscope (TEM, JEM-ARM200F) equipped with energy-dispersive X-ray spectroscopy (EDX). Raman spectra was recorded on LabRAM Aeamis microscopic confocal Raman spectrometer (Horiba Jobin Yivon) to analyze the carbon outer coating with excitation wavelength of 325 nm.

All of the electrocatalytic characterizations for ORR were performed on Autolab PGSTAT204 electrochemical workstation in 0.1 M KOH solution. A three-electrode system consisted of glassy carbon working electrode with a diameter of 5 mm, Pt foil counter electrode and Ag/AgCl reference electrode was employed. To prepare the working electrode, 5 mg of AlN@C nanocomposites should be dispersed in the mixture of 1400 μL of isopropanol, 600 μL of ultrapure water and 30 μL of Nafion solution (5.0 wt%) by ultrasonic processing for 30 min to form the catalyst ink. Then, 20 μL of ink was pipetted onto the surface of glassy carbon electrode with a catalyst loading of ~0.25 mg cm^{-2}. Cyclic voltammetry (CV) measurements were carried out at a scan rate of 50 mV s^{-1} from -0.8 to 0.2 V versus Ag/AgCl in N_2 or O_2-saturated 0.1 M KOH solution. The rotating disk electrode (RDE) measurements were conducted at a scan rate of 10 mV s^{-1} with the rotation rate of 400, 800, 1200, 1600 and 2000 rpm. Chronoamperometry I-t curve was recorded with the rotation rate of 1600 rpm in O_2-saturated electrolyte on -0.4 V versus Ag/AgCl, and 3 M methanol could be added at 500 s for the test of methanol-tolerance. Before the experiments, all electrodes should be activated by potential cycling from -0.8 to 0.2 V at a scan rate of 500 mV s^{-1}. As a comparison, the working electrodes modified by commercial AlN and Pt/C catalysts were prepared and tested in the same way.

III. Results and Discussion

The structural characterizations of the carbon supported AlN nanocomposites are firstly verified by XRD pattern. As shown in Fig. 1, the typical diffraction peaks located at 2-theta = 33.2, 36.0, 37.9, 49.8, 59.3, 66.1, 69.7, 71.4, 72.6 and 81.1° corresponding well to the hexagonal AlN phase (ICDD-PDF No. 25 – 1133). The sharp and strong peaks indicate the high crystallization of AlN. Meanwhile, a relative soft and weak peak around 26.0° is obvious, which can be indexed as graphite carbon (ICDD-PDF No. 41 – 1487). All XRD characterizations suggest that the as-prepared sample is consisted of AlN and graphite carbon.

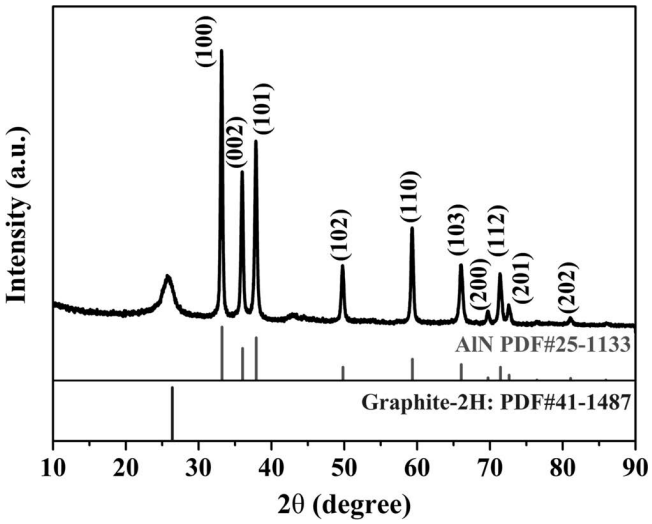

Fig. 1: XRD pattern of AlN@C nanocomposites.

To investigate the micro- structure and morphology of the composites, scanning electron microscopy (SEM) image exhibited the AlN nanoparticles and graphite carbon outer layer in Fig. 2a. For more detailed characterizations, TEM and HRTEM images at different magnifications are shown in Fig. 2b-d. It can be observed that massive graphite carbon encloses the AlN nanoparticles with an average size of ~25 nm, and the nanocomposites are stacked disorderly. The average particle size is in agreement with the calculated result according to Scherrer equation from the main diffraction peaks (24.6 nm), and the lattice spacing of 0.246 nm corresponds to the (002) crystal planes of AlN. Furthermore, the elemental mapping images in Fig. 3 show uniform spatial distribution of C, Al and N, and the atomic ratio of Al and N can be evaluated to be ~1 according to the EDX spectrum in Fig. 4.

In order to characterize the graphite carbon outer coating, Raman spectra of the nanocomposites is shown in Fig. 5. The curve conforms to typical Raman spectra of graphite carbon with high graphitization level. The Raman peaks at 1586 cm^{-1} corresponds to G band that is attributed to sp^2 hybridization of carbon atoms, and another broad peak at 1410 cm^{-1} can be assigned to D band of the

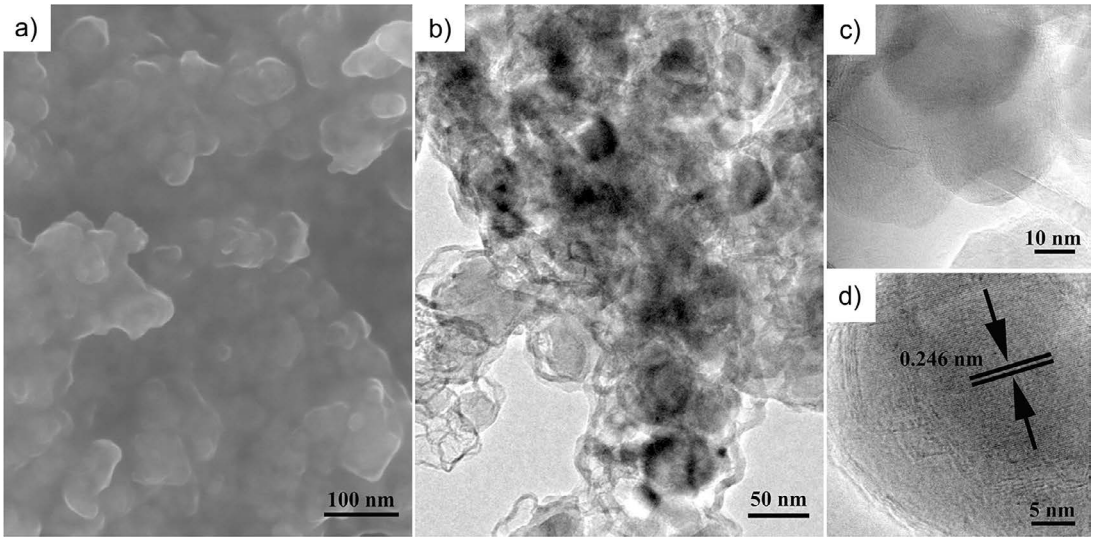

Fig. 2: SEM image (a), TEM images (b, c) at different magnifications and HRTEM image (d) of AlN@C nanocomposites.

local defects and disorders. It should be pointed out that the obvious shifts of D band can be attributed to the disorders of N- substituted and the adsorption towards metal nitrides [31, 32]. Thus, the AlN@C nanocomposites can be accurately identified as the AlN nanoparticles enclosed by graphite carbon.

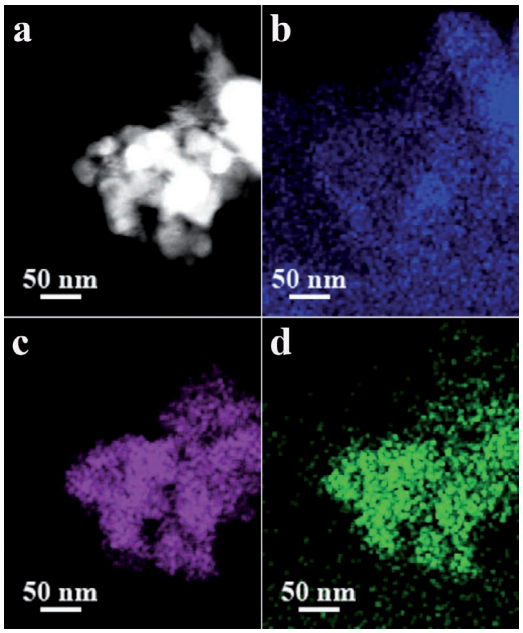

Fig. 3: HR-TEM image (a) and element mapping spectra C (b), Al (c) and N (d) of AlN@C nanocomposites.

As previously reported, NH_3 and some chemically reactive hydrogen-, carbon-, and nitrogen-containing atomic species such as CN_2^{2+}, $C_2N_2^+$, $C_3N_2^+$ and $C_3N_3^+$ can be released during the pyrolysis of melamine at appropriate temperature. These chemically reactive atomic species reduce aluminium oxide to aluminum elements and the N atoms can be incorporation into the metal lattice at high temperature with the high purity nitrogen shielded. Meanwhile, the graphite carbon outer layers are produced with the synergistic effect of AlN nanoparticles [33].

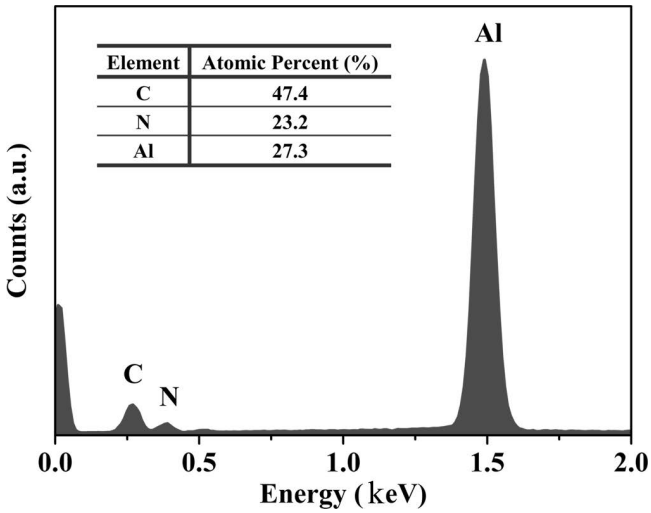

Fig. 4: EDX measurements of AlN@C nanocomposites.

The electrocatalytic activities of AlN@C nanocomposites for the ORR are firstly characterized by CV tests as shown in Fig. 6. Comparing with the featureless CV curve obtained in N_2-saturated electrolyte, both AlN@C nanocomposites and commercial AlN exhibit typical reductions current peak in O_2-saturated condition, which suggests the intrinsic electrochemical property of AlN as an ORR catalyst. Obviously, AlN@C nanocomposites present higher current density than commercial AlN, indicating the better ORR catalytic activity for synergistic effect of the graphite carbon outer coating. In addition, the ORR kinetics of AlN@C nanocomposites and commercial AlN are further investigated by linear sweep voltammetry (LSV) tests with increasing electrode rotation rates from 400 to 2000 rpm, and the Koutecky-Levich (K-L) plots at different potentials are also presented in Fig. 7. It is easy to find that the current density is enhanced with the rotation rate of both samples, while the limited diffusion current density of AlN@C nanocomposites is apparently higher than that of commercial AlN at the same rotation rate. As the key parameter to estimate ORR kinetics, the number of transferred electron (n) of AlN@C nanocomposites is

calculated to be 2.23 to 2.43 according to the slops of K-L plots, indicating the mixed process of 2- and 4- electrons transfer during the oxygen reduction. However, the number of transferred electron of AlN is limited at 1.47 to 1.77, which is identified as a sluggish 2-electron peroxide pathway. The favorable promotion in transferred electrons number and pathway can be attributed to the introduction of graphite carbon outer coating, which possesses good electrical conductivity and electrochemical capability [34].

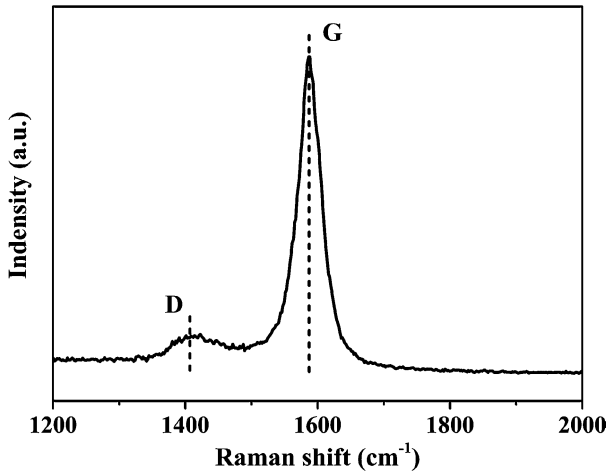

Fig. 5: Raman spectrum of AlN@C nanocomposites from Raman shift of 1200 to 2000 cm^{-1}.

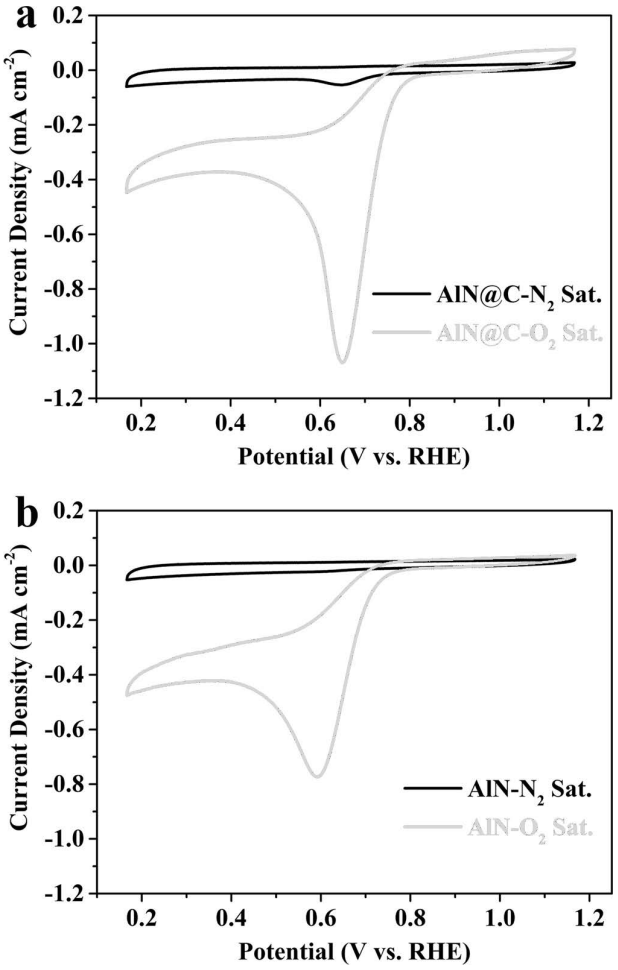

Fig. 6: CV curves of AlN@C nanocomposites (a) and commercial AlN (b) modified glassy carbon RDE in N_2- and O_2- saturated 0.1 M KOH at a scan rate of 50 mV s^{-1}.

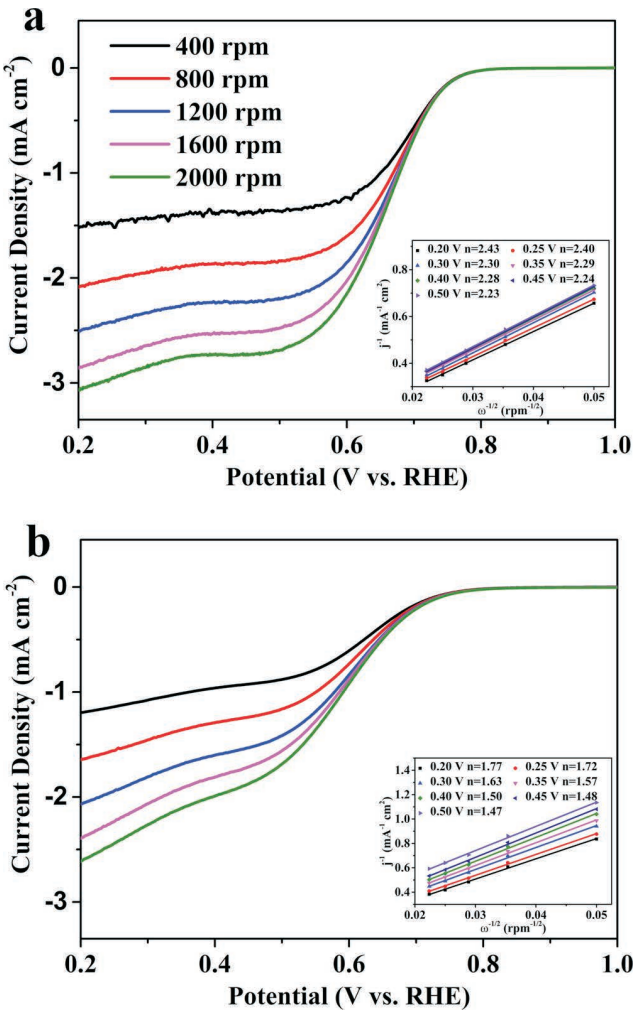

Fig. 7: LSV curves of AlN@C nanocomposites (a) and commercial AlN (b) modified glassy carbon RDE in O_2-saturated 0.1M aqueous KOH electrolyte at a scan rate of 5 mVs^{-1} from 400 to 2000 rpm, and the insets showed linear fitting of the Koutecky-Levich model at different potentials.

Moreover, the ORR polarizations curves of different catalysts at the rotation rate of 1600 rpm exhibits a visualized comparison for their electrocatalytic ability. As shown in Fig. 8, the ORR onset potentials of AlN@C nanocomposites and commercial AlN are 0.82 and 0.76 V, and half-wave potential are 0.66 and 0.57 V vs. RHE, respectively. Although there is a certain gap between the best ORR catalyst of Pt/C and AlN@C nanocomposites, the virtual improvement for the composites with graphite carbon outer coating is of great significance. The novel graphite carbon supported AlN@C nanocomposites provide an unprecedented application to promote the cathodic oxygen reduction for the kind of traditional ceramic material. Besides that, the crossover of methanol is a serious constraint for the practical application in DMFCs. Fig. 9a shows the methanol-tolerant ability in term of chronoamperometric curves by adding 3 M methanol at 500 s. It is clear that a remarkable change in the current density can be observed for Pt/C catalyst as the addition of methanol, while no noticeable change can be found for the catalysts of commercial AlN and AlN@C nanocomposites. These results demonstrate that AlN is much less

active towards methanol oxidation reaction, which contributes to the tolerance performance of methanol in the ORR process. In order to investigate internal factors for the notable methanol-tolerance, CV tests with and without methanol are recorded (Fig. 9b). Compared with the typical CV curves obtained in O_2-saturated electrolyte without methanol, no oxidation or reduction current peak can be observed. However, the commercial AlN suffers a severe decrease in ORR current density and onset potential. Thus, we determine that the intrinsic stability cooperating with the outer coating of graphite carbon results in the enhanced methanol-tolerant ability of AlN@C nanocomposites.

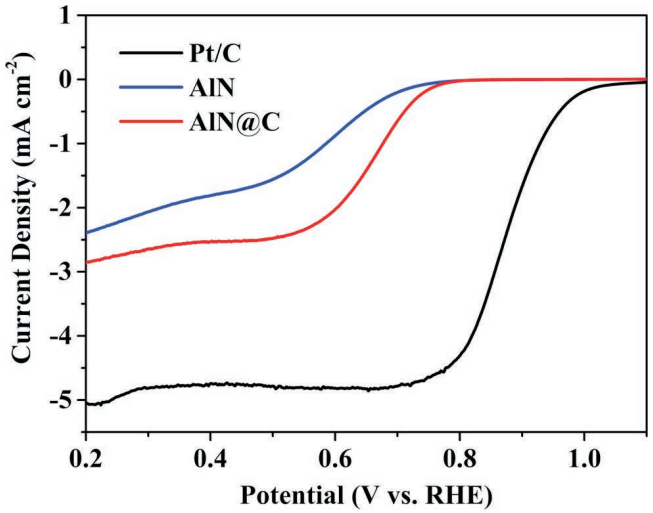

Fig. 8: ORR polarization curves of Pt/C, AlN@C nanocomposites and commercial AlN modified glassy carbon RDE at1600 rpm in O_2-saturated 0.1 M KOH electrolyte.

In addition, the chronoamperometric curves are also used to test the long-time durability of the catalysts. As shown in Fig. 10, the current densities of Pt/C, commercial AlN and AlN@C nanocomposites electrodes remain 87.3, 70.4 and 91.4 percentage of their initial values after 10000 s. The commercial AlN without graphite carbon outer coating displays a poor durability, and that is caused by the possible catalyst dissolution on surface of electrode. Therefore, the remarkable enhanced durability of as-prepared AlN@C nanocomposites can be attributed to the protector of graphite carbon, which is chemically stable in alkaline condition and can effectively insulate the corrosion from KOH electrolyte [35].

In terms of the above analyses of ORR electrocatalytic performance, the AlN@C nanocomposites consisted of AlN nanoparticles and graphite carbon outer coating display the higher current density, more positive onset and half-wave potentials, fine methanol tolerance, and enhanced long-time durability than commercial AlN. We deduce that the graphite carbon outer coating acts as the electrical conduction layer to enhance the charge transportation in the ORR process and the protector to prevent the catalysts poisoning.

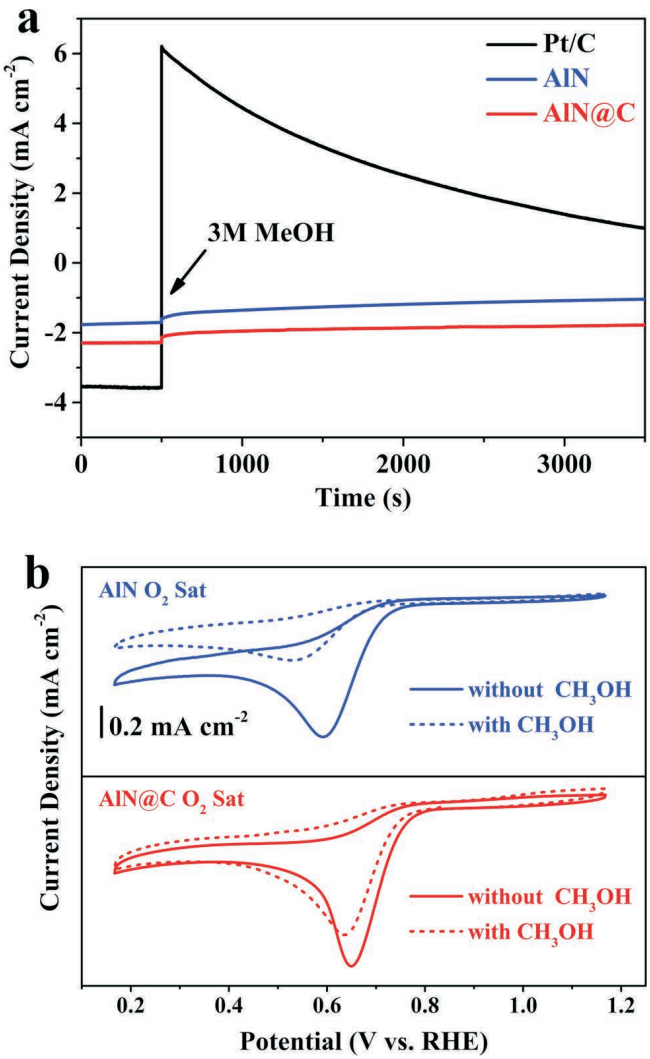

Fig. 9: (a) Chronoamperometric response of Pt/C, AlN@C nanocomposites and commercial AlN modified glassy carbon RDE at 0.4 V in O_2-saturated 0.1 M KOH with 1600 rpm, 3 M methanol was injected after 500 s; (b) CV curves of AlN@C nanocomposites (downside) and commercial AlN (upside) modified glassy carbon RDE in O_2-saturated 0.1 M KOH at a scan rate of 50 mV s^{-1} with or without 3 M methanol.

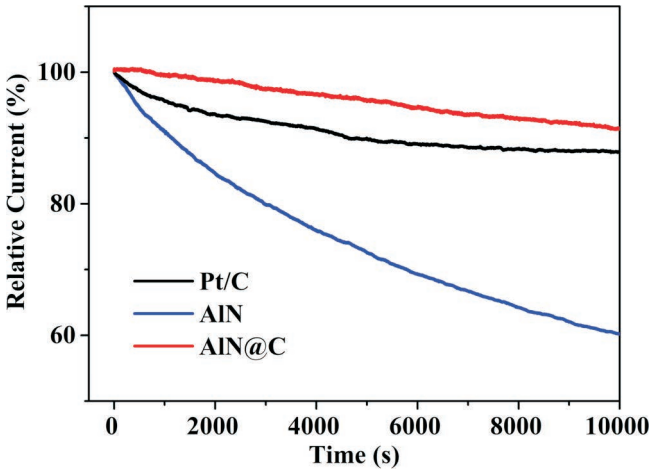

Fig. 10: Chronoamperometric curves of Pt/C, AlN@C nanocomposites and commercial AlN modified glassy carbon RDE at 0.4 V in O_2-saturated 0.1 M KOH electrolyte with 1600 rpm.

IV. Conclusions

In summary, the novel AlN@C nanocomposites of AlN nanoparticles enclosed by graphite carbon outer coating were synthesized via a one-step solid-state method. Their electrochemical performance towards catalyzing ORR, which with little attention in the previous reports, has been investigated in this work. AlN@C nanocomposites exhibit positive onset potential, half-wave potential and higher current density than commercial AlN, which can attribute to the unique features of graphite carbon outer coating. Although the ORR activity cannot match that of Pt/C catalyst, the AlN@C nanocomposites exhibit superior methanol-tolerant ability and good durability. All of these performances make the AlN@C nanocomposites a promising methanol-tolerant catalyst for alkaline DMFCs and other applications.

Acknowledgment

This work was financially supported by the opening fund of Key Laboratory of Silicon Device Technology, Chinese Academy of Sciences, and National Natural Science Foundation of China (Grant nos. 61574020, 51572032, 61674019, 51472221, 51472033, 51472196), and Program for Science &Technology Innovation Talents in Universities of Henan Province (Grant nos. 14HASTIT018).

References

1 Formal, F.L., Bourée, W.S., Prévot, M.S., Sivula, K.: Challenges towards economic fuel generation from renewable electricity: the need for efficient electro-catalysis, Chim. Int. J. Chem., **69**, 789 – 798, (2015).

2 Xie, J., Xie, Y.: Transition metal nitrides for electrocatalytic energy conversion: opportunities and challenges, Chem. - A Eur. J., **22**, 3588 – 3598, (2016).

3 Hong, W.T., Risch, M., Stoerzinger, K.A., Grimaud, A., Suntivich, J., Shao-Horn, Y.: Toward the rational design of non-precious transition metal oxides for oxygen electrocatalysis, Energy Environ. Sci., **0**, 1 – 3, (2013).

4 Debe, M.K.: Electrocatalyst approaches and challenges for automotive fuel cells, Nature, **486**, 43 – 51, (2012).

5 Guo, Y.G., Hu, J.S., Wan, L.J.: Nanostructured materials for electrochemical energy conversion and storage devices, Adv. Mater., **20**, 2878 – 2887, (2008).

6 Zhang, Z., Liu, J., Gu, J.: An overview of metal oxide materials as electrocatalysts and supports for polymer electrolyte fuel cells, Energy Environ. Sci., **7**, 2535, (2014).

7 Gröger, O., Gasteiger, H.A., Suchsland, J.P.: Review-electromobility: Batteries or fuel cells? J. Electrochem. Soc., **162**, A2605-A2622, (2015).

8 Xia, B.Y., Yan, Y., Li, N., Wu, H.B., Lou, X.W., Wang, X.: A metal-organic framework-derived bifunctional oxygen electrocatalyst, Nat. Energy., **1**, 15006, (2016).

9 Liu, H., Song, C., Zhang, L., Zhang, J., Wang, H., Wilkinson, D.P.: A review of anode catalysis in the direct methanol fuel cell, J. Power Sources, **155**, 95 – 110, (2006).

10 Lei, M., Wang, J., Li, J.R.,Wang, Y.G., Tang, H.L., Wang, W.J.: Emerging methanol-tolerant AlN nanowire oxygen reduction electrocatalyst for alkaline direct methanol fuel cell, Sci. Rep., **4**, 6013, (2014).

11 Cao, J., Guo, M., Wu, J., Xu, J., Wang, W., Chen, Z.: Carbon-supported Ag@Pt core-shell nanoparticles with enhanced electrochemical activity for methanol oxidation and oxygen reduction reaction, J. Power Sources, **277**, 155 – 160, (2015).

12 Yeh, P., Chang, C.H., Shih, N., Yeh, N.: Durability and efficiency tests for direct methanol fuel cell's long-term performance assessment, Energy, **107**, 716 – 724, (2016).

13 Ge, X., Sumboja, A., Wuu, D., An, T., Li, B., Goh, F.W.T., Hor, T.S.A., Zong, Y., Liu, Z.: Oxygen reduction in alkaline media: from mechanisms to recent advances of catalysts, ACS Catal., **5**, 4643 – 4667, (2015).

14 Zhang, J., Sasaki, K., Sutter, E., Adzic, R.R.: Stabilization of platinum oxygen-reduction electrocatalysts using gold clusters, Science, **315**, 220 – 222, (2007).

15 Huang, Q., Yang, H., Tang, Y., Lu, T., Akins, D.L.: Carbon-supported Pt-Co alloy nanoparticles for oxygen reduction reaction, Electrochem. Commun., **8**, 1220 – 1224, (2006).

16 Choi, S.I., Xie, S., Shao, M., Odell, J.H., Lu, N., Peng, H.C., Protsailo, L., Guerrero, S., Park, J., Xia, X., Wang, J., Kim, M.J., Xia, Y.: Synthesis and characterization of 9 nm Pt-Ni octahedra with a record high activity of 3.3 A/mg_{Pt} for the oxygen reduction reaction,. Nano Lett., **13**, 3420 – 3425, (2013).

17 Chung, Y.H., Chung, D.Y., Jung, N., Park, H.Y., Sung, Y.E., Yoo, S.J.: Effect of surface composition of Pt-Fe nanoparticles for oxygen reduction reactions, Int. J. Hydrogen Energy, **39**, 14751 – 14759, (2014).

18 Liu, J., Xu, C., Liu, C., Wang, F., Liu, H., Ji, J., Li, Z.: Impact of Cu-Pt nanotubes with a high degree of alloying on electro-catalytic activity toward oxygen reduction reaction, Electrochim. Acta., **152**, 425 – 432, (2015).

19 Malacrida, P., Escudero-Escribano, M., Verdaguer-Casadevall, A., Stephens, I.E.L., Chorkendorff, I.: Enhanced activity and stability of Pt-La and Pt-Ce alloys for oxygen electroreduction: the elucidation of the active surface phase, J. Mater. Chem. A, **2**, 4234 – 4243, (2014).

20 Jung, N., Chung, D.Y., Ryu, J., Yoo, S.J., Sung, Y.E.: Pt-based nanoarchitecture and catalyst design for fuel cell applications, Nano Today, **9**, 433 – 456, (2014).

21 Chen, Z., Higgins, D., Yu, A., Zhang, L., Zhang, J.: A review on non-precious metal electrocatalysts for PEM fuel cells, Energy Environ. Sci., **4**, 3167, (2011).

22 Bezerra, C.W.B, Zhang, L., Lee, K., Liu, H., Marques, A.L.B., Marques, E.P., Wang, H., Zhang, J.: A review of Fe-N/C and Co-N/C catalysts for the oxygen reduction reaction, Electrochim. Acta., **53**, 4937 – 4951, (2008).

23 Lin, S., Bi, K., Pan, X., Hao, Y., Du, Y., Liu, J., Fan, D., Wang, Y., Lei, M.: A one-step way to novel carbon-niobium nitride nanoparticles for efficient oxygen reduction, J. Am. Ceram. Soc., **100**, 638 – 646, (2017).

24 Wang, Y., Ohnishi, R., Yoo, E., P. He, Kubota, J., Domen, K., Zhou, H.: Nano- and micro-sized TiN as the electrocatalysts for ORR in Li-air fuel cell with alkaline aqueous electrolyte, J. Mater. Chem., **22**, 15549, (2012).

25 Guo, S., Dong, S.: Graphene nanosheet: synthesis, molecular engineering, thin film, hybrids, and energy and analytical applications, Chem. Soc. Rev., **40**, 2644 – 2672, (2011).

26 Chung, H.T., Won, J.H., Zelenay, P.: Active and stable carbon nanotube/nanoparticle composite electrocatalyst for oxygen reduction, Nat. Commun., **4**, 1922, (2013).

27 Li, Y., Li, Y., Zhu, E., McLouth, T., Chiu, C.Y., Huang, X., Huang, Y.: Stabilization of high performance ORR Pt electrocatalyst supported on reduced graphene oxide (RGO)/carbon black (CB) Composite, J. Am. Chem. Soc., **134**, 12326 – 12329, (2012).

28 Lota, G., Fic, K., Frackowiak, E.: Carbon nanotubes and their composites in electrochemical applications, Energy Environ. Sci., **4**, 1592, (2011).

29 Huang, K., Bi, K., Liang, C., Lin, S., Zhang, R., Wang, W.J., Tang, H.L., Lei, M.: Novel VN/C nanocomposites as methanol-tolerant oxygen reduction electrocatalyst in alkaline electrolyte, Sci. Rep., **5**, 11351, (2015).

[30] Meng, F.L., Wang, Z.L., Zhong, H.X., Wang, J., Yan, J.M., Zhang, X.B.: Reactive multifunctional template-induced preparation of Fe-N-doped mesoporous carbon microspheres towards highly efficient electrocatalysts for oxygen reduction, Adv. Mater., **28**, 7948 – 7955, (2016).

[31] Ferrari, A.C., Raman spectroscopy of graphene and graphite: Disorder, electron-phonon coupling, doping and nonadiabatic effects, Solid State Commun., **143**, 47 – 57, (2007).

[32] Pimenta, M.A., Dresselhaus, G., Dresselhaus, M.S., Cançado, L.G., Jorio, A., Saito, R.: Studying disorder in graphite-based systems by Raman spectroscopy, Phys. Chem. Chem. Phys., **9**, 1276 – 1291, (2007).

[33] Jürgens, B., Irran, E., Senker, J., Kroll, P., Müller, H., Schnick, W.: Melem (2, 5, 8-Triamino-tri-s-Triazine), an important intermediate during condensation of melamine rings to graphitic carbon nitride: synthesis, structure determination by x-ray powder diffractometry, Solid-State NMR, and Theoretical Studies, J. Am. Chem. Soc., **125**, 10288 – 10300, (2003).

[34] Chen, J., Zou, G., Zhang, Y., Song, W., Hou, H., Huang, Z., Liao, H., Li, S., Ji, X.: Activated flake graphite coated with pyrolysis carbon as promising anode for lithium storage, Electrochim. Acta., **196**, 405 – 412, (2016).

[35] Hu, Y., Jensen, J.O., Zhang, W., Cleemann, L.N., Xing, W., Bjerrum, N.J., Li, Q.: Hollow spheres of Iron carbide nanoparticles encased in graphitic layers as oxygen reduction catalysts, Angew. Chem. Int. Edit., **53**, 3675 – 3679, (2014).